

LMCX-4: the optical 30-day cycle and its implications[★]

S.A. Ilovaisky¹, C. Chevalier¹, C. Motch¹, M. Pakull², J. van Paradijs³, and J. Lub⁴

¹ Observatoire de Besançon, 41 bis avenue de l'Observatoire, F-25044 Besançon Cedex, France

² Institut für Astronomie und Astrophysik, Technische Universität Berlin, D-1000 Berlin

³ Astronomical Institute “Anton Pannenoek”, University of Amsterdam, NL-1018 WB Amsterdam, The Netherlands

⁴ Leiden Observatory, Postbus 9513, NL-2300 RA Leiden, The Netherlands

Received March 22, accepted June 14, 1984

Summary. Analysis of an extensive set of optical photometry of the massive X-ray binary LMCX-4 obtained at ESO from 1976 through 1983 shows the presence of the X-ray 30-day cycle discovered by Lang et al. (1982). The periodogram exhibits peaks at the sums of the orbital and half-orbital frequencies with the 30-day frequency and at the 30-day frequency itself. During X-ray OFF states, the amplitude of the 1.408-day orbital period double-wave light curve is 0.07 mag, while during ON states it increases to 0.20 mag. We explain the observed effects in terms of an X-ray illuminated, tilted, counter-“precessing” accretion disk. The excess light comes both from the accretion disk itself and from the illuminated hemisphere of the primary, the latter experiencing variable X-ray shadowing due to the changing aspect of the disk. Each source contributes approximately half of the observed excess. The long-term behavior observed in LMC X-4 resembles that of Her X-1, suggesting the same basic underlying clock mechanism is at work in both systems.

Key words: binary X-ray sources – accretion disks

1. Introduction

The binary X-ray source LMCX-4, the second to be discovered in an external galaxy, exhibits a large degree of variability. Described as possibly variable on the basis of early UHURU data (Leong et al., 1971), it was not detected with OSO-7 (Markert and Clark, 1975) nor with Copernicus (Rapley and Tuohy, 1974), but was seen again with the Ariel 5 SSI (Griffiths and Seward, 1977) and SAS-3RMC experiments (Epstein et al., 1977). During the latter observation, the source showed flaring behaviour. A small RMC error box stimulated a search for an optical identification (Pakull, 1977; Sanduleak and Philip, 1977; Hiltner, 1977; Chevalier and Ilovaisky, 1977, hereinafter referred to as CI77). Photometric observations (CI77) of an early-type star in the Large Magellanic Cloud found by Sanduleak and Philip led to the discovery of a 1.4 d periodic modulation. Soon thereafter, X-ray eclipses with that period were found in the SAS-3 and Ariel 5 data (White, 1978; Li et

al., 1978). The first HEAO-1 observations (Skinner et al., 1980) showed strong X-ray variability on a time scale of month, thus explaining the early non-detections. Analysis of the complete HEAO-1 500-d data base (Lang et al., 1981) demonstrated the X-ray flux to be modulated with a 30-d period. More recently, SAS-3 data obtained during flaring episodes (Kelley et al., 1982) revealed X-ray pulsations with a 13.5 s period.

The early optical observations of 1977 showed a very large amplitude ellipsoidal-type light curve with variability near orbital phase $\phi_{orb} = 0.75$ on a time scale of two weeks (CI77). In an effort to understand the underlying causes of both the large amplitude and the variability, suspected to be the consequence of an X-ray to optical luminosity ratio of order unity, we undertook a long-term project of photometric monitoring. Here we present a detailed analysis of the optical photometry obtained at ESO from 1976 through 1983 which demonstrates that the light curve amplitude is modulated with the 30-d X-ray period. We show that the observed behavior can be accounted for, as in the case of the Her X-1/Hz Her system (Gerend and Boynton, 1976; Petterson 1977) in terms of an X-ray heated, tilted, counter-“precessing”¹ accretion disk casting an X-ray shadow on the illuminated facing hemisphere of the companion. An early account of this work was presented elsewhere (Chevalier et al., 1981). Other similar long-period modulations, which could be also due to such “precessing” disks, have been reported in CygX-1 (Priedhorsky et al., 1982; Kemp et al., 1983) and possibly in 4U1907 + 09 (Priedhorsky and Terrell, 1983).

2. The observations

The photometric observations presented here, the amalgam of results from many observers, were obtained at the European Southern Observatory, La Silla, Chile with several telescopes (50 cm, 61 cm, 90 cm, 1 m, 1.52 m, 1.54 m, and 3.6 m) over the period 1976 to 1983.

With the exception of the observations made at the Dutch 90 cm, which were made in the Walraven system, all other data are in the Johnson UB system. Standard-star observations allowed absolute calibration of most runs; however, for some data sets only differential photometry was available and, before merging all data,

Send offprint requests to: S.A. Ilovaisky

[★] Based on observations collected at the European Southern Observatory, La Silla, Chile

¹ We use here the term “precession” to describe *apparent* precession, not real *forced* precession (see Crosa et al., 1980)

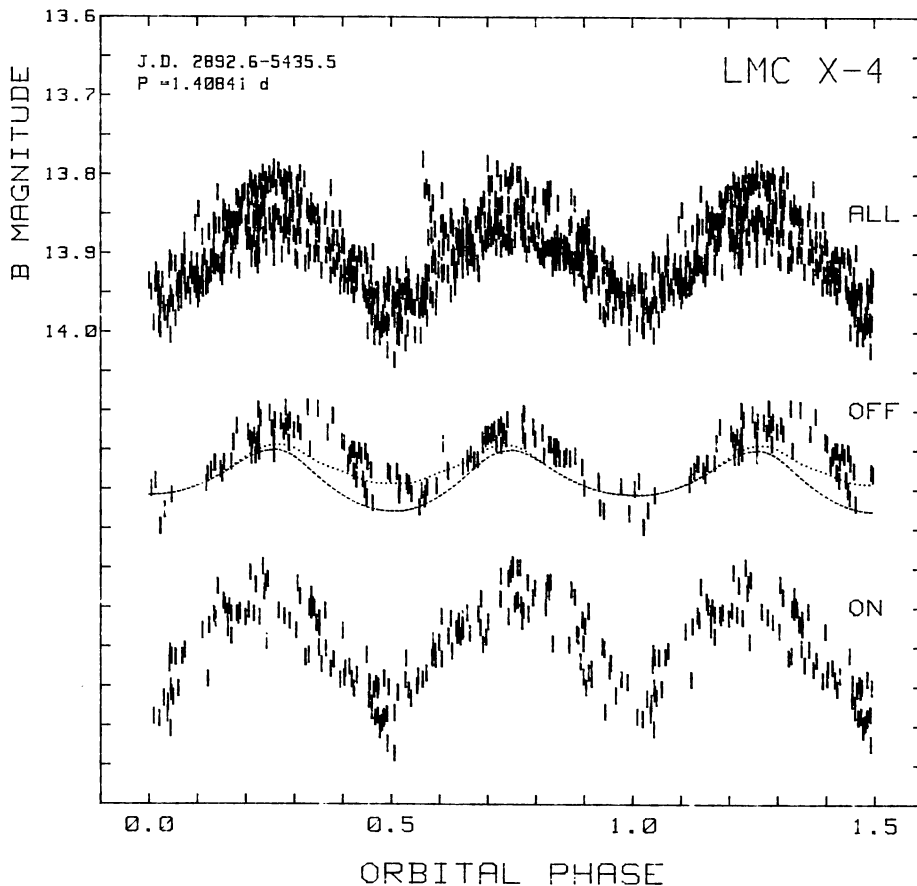


Fig. 1. Optical B -band photometric data of the LMC X-4 optical counterpart obtained at ESO during the years 1976–1983 plotted as a function of 1.408-d orbital phase. Representative ± 0.01 mag error bars are shown. (a) Top: All data. (b) Middle: Data corresponding to the X-ray OFF phase (30-d cycle phases 0.9–0.1). Also shown are two model light curves discussed in the text: The dashed curve is the pure ellipsoidal model while the dotted curve is fitted to the data near $\phi_{\text{orb}} = 0.5$ by adding a suitable amount of X-ray heating. Curve is shifted by 0.25 mag with respect to (a). (c) Bottom: Data corresponding to the X-ray ON phase (30-d phases 0.35–0.6). Curve is shifted by 0.25 mag with respect to (b)

corrections were applied derived from matching average magnitudes at orbital phase $\phi_{\text{orb}} = 0.0$ and/or from matching characteristic features in the light curve with a master template derived from all data. The Johnson B -band data (730 data points) show the highest signal-to-noise ratio and can be merged for analysis with low risk. The Johnson V -band data, showing a poorer signal-to-noise ratio, will not be further analyzed here, except in so far as they will be used to derive $B-V$ colors. Johnson U -band data are of a quality equal to the B data but as no equivalent is available in the Walraven system the data base is smaller. In what follows we analyze the B -band data.

3. Orbital period redetermination

In Figure 1 we have plotted all B data using the ephemeris given below. Standard ± 0.01 mag error bars have been drawn for all data points. This is certainly not representative of the external accuracy of all runs, but we shall adopt it in what follows. There is clear indication of variability at all phases, with the exception of the region near $\phi_{\text{orb}} = 0.0$. In fact, the kind of variability seen here (most visible near the peaks $\phi_{\text{orb}} = 0.25$ and 0.75), and which is related to the 30-d X-ray period, was already present in the early photometric data (CI77), although only around the maximum at $\phi_{\text{orb}} = 0.75$.

The B data shown in Figure 1, spanning a base-line of 2543 d, were analyzed using signal-folding techniques to derive an improved value for the orbital period, with the observations averaged in 20 min time bins. We find $P_{\text{orb}} = 1.40841 \pm 0.00001$ d with $\text{JD} 2444956.65 \pm 0.01$ as the epoch for orbital phase zero. This

period agrees well with that derived from radial velocity measurements (1.40830 ± 0.00050 d, Hutchings et al., 1978), and with that derived from HEAO-1 X-ray observations (1.40839 ± 0.00010 d, Lang et al., 1981) covering an interval of 500 d. Kelley et al. (1982) give 1.40832 ± 0.00005 d and $\text{JD} 2442829.994 \pm 0.019$ based on pulse timings and a re-analysis of all X-ray data. Again these results are consistent with ours. In what follows we adopt the following orbital ephemeris:

$$\phi_{\text{orb}} = 0.0 \quad \text{for} \quad \text{JD} 2444956.65 + 1.40841 * n.$$

4. Optical evidence for the 30-day period

The B data have been subjected to least squares frequency analysis techniques (Lomb, 1976; Motch, 1979). In Fig. 2c we show the periodogram of the raw data which exhibits a strong main peak at twice the orbital frequency $2 * f_{\text{orb}} = 1.420 \text{ d}^{-1}$, with side-band structure introduced by the window function, (i.e., the distribution of the data in time). No peak appears in Fig. 2b at the orbital frequency itself ($f_{\text{orb}} = 0.710 \text{ d}^{-1}$), as the basic modulation is a sine wave at half the orbital period (doubled-waved light curve) and our technique searches for periods by adjusting sines and cosines. The frequency spacing between the side-bands is consistent with the underlying yearly (or nearly so) natural recurrence period between observing runs. After removal of the dominant modulation at $2 * f_{\text{orb}}$, the periodogram (see Fig. 2f) exhibits a significant secondary peak at $f_1 = 1.453 \text{ d}^{-1}$ with the expected window function side-bands (only two are clearly visible). Further removal of this frequency yields a rather flat periodogram. In Fig. 2e,

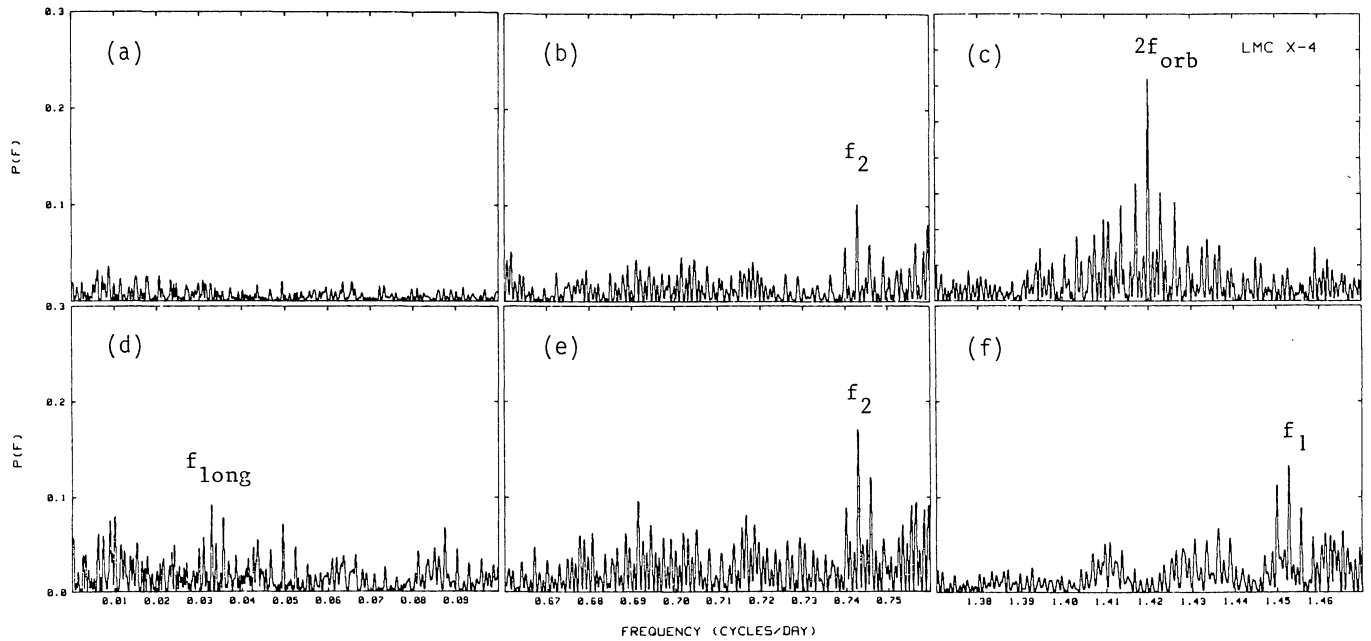


Fig. 2a–f. Parts of the periodogram of the *B*-band data for LMCX-4. TOP panel: periodogram of the raw data around the 30-d frequency f_{long} (a left), the orbital frequency f_{orb} (b center) and the half-orbital frequency $2*f_{\text{orb}}$ (c right). Note the vertical scale change for (c). BOTTOM panel: the periodogram for the same frequency windows (d–f) after demodulation at the dominant half-orbital frequency, $2*f_{\text{orb}}$. The peaks at f_1 and f_2 are the frequency sums described in the text: $f_1 = 2*f_{\text{orb}} + f_{\text{long}}$ and $f_2 = f_{\text{orb}} + f_{\text{long}}$

although no peak is present near f_{orb} , a secondary peak (with two side-bands) appears near $f_2 = 0.743 \text{ d}^{-1}$. This peak remains present after removal of the underlying modulations at $2*f_{\text{orb}}$ and f_1 . After demodulation at $2*f_{\text{orb}}$ a small but significant peak appears in the periodogram at $f_{\text{long}} = 0.033 \text{ d}^{-1}$ (Fig. 2d). The implications of this peak will be discussed later.

The secondary peaks appearing at the frequencies f_1 and f_2 are the *sums* of the orbital and half-orbital frequencies with the 30-day frequency: $f_1 = 2*f_{\text{orb}} + f_{\text{long}}$ and $f_2 = f_{\text{orb}} + f_{\text{long}}$. Using our value for the orbital period, these secondary frequencies yield two independent estimates of f_{long} , whose average value, based on 83 cycles, gives:

$$P_{\text{long}} = 30.40 \pm 0.03 \text{ d}$$

in agreement with the value derived from X-rays ($30.48 \pm 0.06 \text{ d}$, Lang et al., 1981), based on just 17 cycles. This value is slightly, but not significantly, different from that derived directly from the peak at f_{long} , $30.50 \pm 0.05 \text{ d}$. We have made the assumption here that the value of the long period is a constant. It would not be surprising to find phase changes, as in Her X-1 (Davison and Fabian, 1974). Unfortunately, the data at hand do not sample the 30-d cycle homogeneously and thus cannot be used to obtain this information.

Note that no peak is found near the frequencies corresponding to the *differences* $2*f_{\text{orb}} - f_{\text{long}}$ and $f_{\text{orb}} - f_{\text{long}}$. The appearance of the long period modulation in the spectrum as frequency *sums* can be interpreted, as in the case of the HZ Her/Her X-1 system (Deeter et al., 1976; Gerend and Boynton, 1976), in terms of variable X-ray shadowing of the primary due to an accretion disk “precessing” in the opposite sense to the orbital motion. The peak appearing at the low frequency f_{long} is due to the optical light contributed by the disk itself, a fact which will be discussed later. Its smaller amplitude is probably related to the inhomogeneous sampling of the 30-d cycle and does not necessarily imply a lesser contribution from the disk.

A new, natural and non-arbitrary phase 0.0 for the 30-d cycle can be defined as the epoch when the optical light curve amplitude is *minimum* (corresponding to the middle of the X-ray OFF phase). This, determined as the time when the modulations at $2*f_{\text{orb}}$ and f_1 are out of phase², yields 2443393.66 ± 0.02 . The phase zero epoch for the modulation whose peak appears at f_{long} is $\text{JD } 2443393.70 \pm 0.06$. This phase definition differs from that adopted for Her X-1 (Gerend and Boynton, 1976) where 0.0 corresponds to X-ray maximum. We suggest adoption henceforth of our phase convention, replacing that of Lang et al. (1981), based simply on the starting time of the HEAO-1 500-d observation. In what follows we use the following 30-d period ephemeris:

$$\phi_{30} = 0.0 \text{ for } \text{JD } 2443393.66 + 30.40 * n.$$

5. Colors

Although a large fraction of the data base contains differential photometric measurements in the Johnson and Walraven bands, several runs included a direct and independent calibration in terms of *UBV* standards. From these sets we have determined the average colors of LMC X-4 to be $B-V = -0.23 \pm 0.01$ and $U-B = -1.04 \pm 0.01$. Assuming a visual extinction of $A_v = 0.16$ (Bonnet-Bidaud et al., 1981), $E_{B-V} = 0.05$ and $E_{U-B} = 0.04$ (for a spectral type O7, Johnson, 1958), the unreddened colors are $(B-V)_0 = -0.28$ and $(U-B)_0 = -1.08$, consistent with a 35,000 K Kurucz (1979) model atmosphere, which predicts $B-V = -0.30$, $U-B = -1.10$. For a primary radius of $R_{\text{opt}} = 8.9 R_{\odot}$ (Kelley et al., 1983) and luminosity $L_{\text{bol}} = 5 \cdot 10^{38} \text{ ergs}^{-1}$ (CI77), the expected black-body temperature

² For this, imagine the 30-d modulation as the result of a beat between the modulations at $2*f_{\text{orb}}$ and f_1

is 37,000 K (see also Hutchings et al., 1978). The observed $U-B$ is in disagreement with the cooler (27,250 K) ultraviolet Kurucz model atmosphere fit of van der Klis et al. (1982), which predicts $B-V = -0.27$, $U-B = -0.98$.

6. Changes in the light curve

In order to emphasize the changes in the light curve we have plotted (in Fig. 1b and c) our data into two broad 30-d cycle bins ($\phi_{30} = 0.35-0.6$ and $\phi_{30} = 0.9-0.1$), corresponding roughly to the states of maximum (ON) and minimum (OFF) X-ray flux (see Fig. 3 of Lang et al., 1982).

The OFF state light curve shown in Figure 1b resembles light curves typical of massive X-ray binaries, such as Vela X-1 (Zuiderwijk et al., 1977), where tidal and rotational distortion of the primary by the compact companion can explain ellipsoidal-type variations with maximum amplitudes of up a few percent (see reviews by Hutchings, 1982 and Ilovaisky, 1982). Such light curves show two different minima per period, with the minimum at $\phi_{\text{orb}} = 0.5$ being deeper, due to increased gravity darkening of the primary around the region near the Lagrangian point. In massive X-ray binary systems where X-ray heating of the companion takes place, the $\phi_{\text{orb}} = 0.5$ minimum tends to fill in and may become the shallower of the two, as in SMCX-1 (van Paradijs, 1978; van Paradijs and Zuiderwijk, 1977). Our OFF state light curve shows an acceptably small amplitude, possibly consistent with an ellipsoidal effect ($A_{0,0} = 0.08 \pm 0.01$ mag) and a filled-in mid-phase minimum ($A_{0,5} = 0.07 \pm 0.01$) which shows that during the OFF state, when no X-rays arrive at Earth, the primary in the LMC X-4 system sees a considerable X-ray flux. This immediately suggests that during the OFF state the Earth lies in the X-ray shadow cast by the accretion disk.

The ON state light curve shown in Fig. 1c is still characterized by two maxima and two minima per period but exhibits a very large mid-orbital phase amplitude ($A_{0,5} = 0.20$ mag) due to excess light near quadratures and to the extra depth of the mid-phase minimum; see Fig. 1a. With respect to the OFF state curve, the excess at quadratures amounts to 0.07 mag and the extra depth of the mid-phase minimum to 0.05 mag. Assuming a probable finite co-inclination, we can attribute some of this excess light to the accretion disk whose contribution just adds to that of the primary at quadratures.

In order to sort out the changes which take place in the light curve as a function of the long cycle, we have plotted in Fig. 3 our B data into ten 30-d period phase bins, starting with the interval $\phi_{30} = 0.0-0.1$. As expected, the low-amplitude curves are restricted to the 30-d phase interval $\phi_{30} = 0.9-0.1$, corresponding to the X-ray OFF state, while the large-amplitude curves are found in the complementary interval $\phi_{30} = 0.3-0.6$, during the X-ray ON state. Although the data are not homogeneously distributed in 30-day phase, there are hints of complex changes taking place in the phase intervals $\phi_{30} = 0.1-0.2$ and $0.8-0.9$. The mid-orbital phase minimum deepens in the phase interval $\phi_{30} = 0.3-0.5$, close to the time of X-ray maximum flux. The significance of these changes will be discussed in the next Section.

7. Model ellipsoidal light curves

Recent studies of the IUE spectra of LMC X-4 and SMC X-1 (Bonnet-Bidaud et al., 1981; van der Klis et al., 1982) have shown the ultraviolet continua of these systems to exhibit the same type of variations seen in the visible region of the spectrum. In the case of LMC X-4, the sketchy ultraviolet light curve, obtained during the

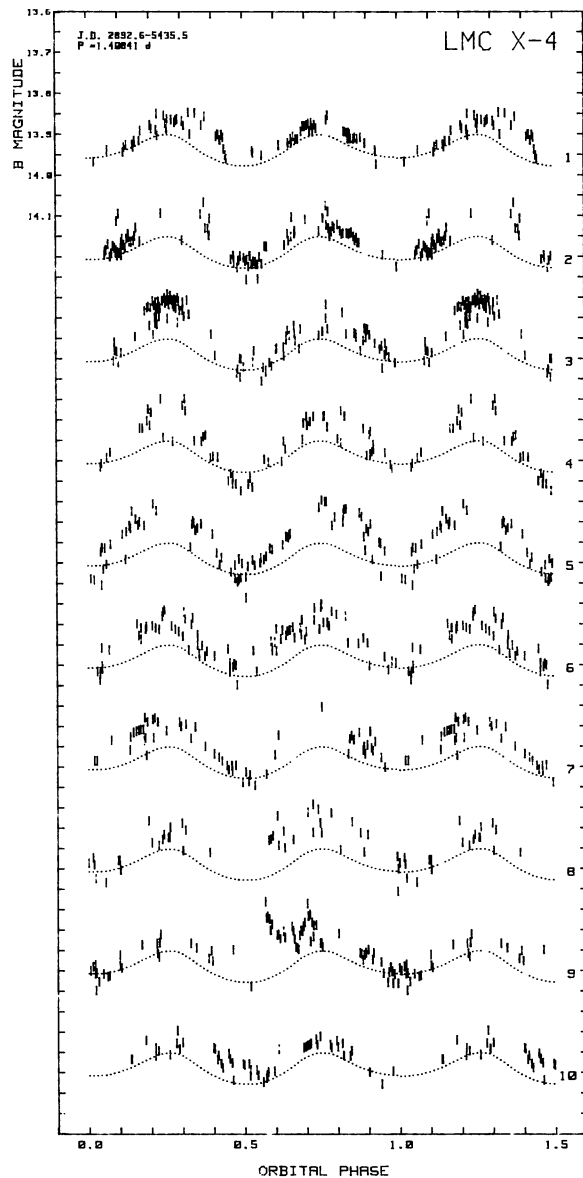


Fig. 3. The B filter data folded with the 1.408-d orbital period and split into 10 elementary light curves each corresponding to a consecutive 30-d cycle phase bin. Curves numbered 1 through 10 correspond to bins $0.0-0.1$, $0.1-0.2$, ..., $0.9-1.0$. The dotted curve superposed onto all light curves as a reference is the pure ellipsoidal model (no heating) discussed in the text and shown in Fig. 1b as the lower dotted line

X-ray OFF states, was fit with a synthetic UV light curve calculated using the code described in Zuiderwijk et al. (1977). The average atmospheric parameters of the primary were obtained from the continuum fit to the ultraviolet spectrum with a Kurucz model atmosphere using $T_{\text{eff}} = 27,250 \pm 2250$ K, $\log g = 4.0$, $L_{\text{bol}} = 5 \cdot 10^{38}$ ergs $^{-1}$ (CI77), $M_x/M_{\text{opt}} = 0.1$, and $i = 75^\circ$.

We have tried to fit to our much higher quality OFF state optical data a synthetic B -band light curve calculated using the same model parameters, minimally modified for $i = 66^\circ$ (Kelley et al., 1983) and $T_{\text{eff}} = 35,000$ K. We adjusted it by setting the value for $\phi_{\text{orb}} = 0.0$ equal to the average of the data set within the orbital phase interval $\phi = 0.97-0.03$: $B = 13.957$ based on 30 data points. This curve, shown in Fig. 1b and in Fig. 3 (where it is adopted henceforth as a fiducial reference), does not fully account for the

OFF state optical data, suggesting that *extra light is still present in the OFF state*. The light dotted line in Fig. 1 b shows the effects of adding a simple heating effect on the primary's facing hemisphere corresponding to $L_x = 1.2 \cdot 10^{38} \text{ ergs}^{-1}$. This indicates that during the OFF X-ray state, when the tilted accretion disk is seen edge-on and no X-rays are seen at Earth, the LMCX-4 primary perceives a sizeable X-ray flux.

We can now evaluate the true excess light at quadratures in the ON-state light curve, with respect to the ellipsoidal model instead of with respect to the OFF-state light curve. This yields an excess of 0.1 mag.

8. A tilted counter-“precession” accretion disk

We have seen in the preceding section that during the X-ray OFF phase the primary sees X-rays, indicating the Earth is in the X-ray shadow cast by the disk. In order for the X-ray shadow to move away, the edge of the disk which is doing the occulting must move down (or up) with a 30-d period relative to the observer; for this to happen the disk needs to change its orientation in space with respect to the observer (it must “precess”) and its rim must be inclined with respect to the orbital plane.

This is the same explanation offered for the 35-d X-ray cycle of Her X-1 (Deeter et al., 1976; Jones and Forman, 1976; Gerend and Boynton, 1976). There the X-ray light curve shows two unequal maxima per 35-d cycle, implying that during the ON state we see the X-ray source from “above” the disk shadow, while during the so-called “short-ON” phase, appearing in the middle of the OFF phase (Jones and Forman 1976), we see the source from “below” (Pettersen, 1977). In the Her X-1 system, where the line of sight is thought to make an 8° angle with respect to the orbital plane (although still subject to debate), the disk appears about 20° thick and it needs to be tilted by 30° with respect to the orbital plane (Gerend and Boynton, 1976).

In LMC X-4 the X-ray curve shows a larger duty cycle, implying the Earth dips “into the X-ray shadow for only 30% of the “precession” period, thereby suggesting a smaller tilt angle. The actual tilt required for the disk is of course also a function of its angular thickness and the observer's co-inclination angle ($90^\circ - i$). Taking the latter to be 24° ($i = 66^\circ$, Kelley et al. 1983), a thickness of $z = 20^\circ$ suggests a tilt angle of about 20° . When the disk is seen as exposed as possible (ON state), the line of sight is inclined by an average of 40° to the disk surface. Conversely, when the observer is in the X-ray shadow (OFF state), the X-ray source is “below” the disk rim but part of the far side of the disk is still visible, although at an incidence of about $10\text{--}15^\circ$.

Precession must take place in a sense *opposite* to the orbital motion in order to explain the existence of the frequency sums $2 \cdot f_{\text{orb}} + f_{\text{long}}$ and $f_{\text{orb}} + f_{\text{long}}$. In Her X-1 most of the observed light comes from the X-ray heated cap of the companion facing the neutron star. The disk casts a shadow on this cap and “precession” moves this shadow around; the primary “sees” all 35-d cycle phases in the course of an orbital period. Similar relative illumination conditions will recur under identical disk-star configurations. The frequency sums show that the recurrence period is *shorter* than the orbital period; the same disk-star configuration is thus reached *earlier*, hence the counter (or retrograde) “precession”.

9. Constant disk-star orientation light curves

In the LMCX-4 system the existence of the frequency sums and the OFF-state filled-in mid-phase minimum show that X-ray illumination of the primary is also far from negligible. To study the

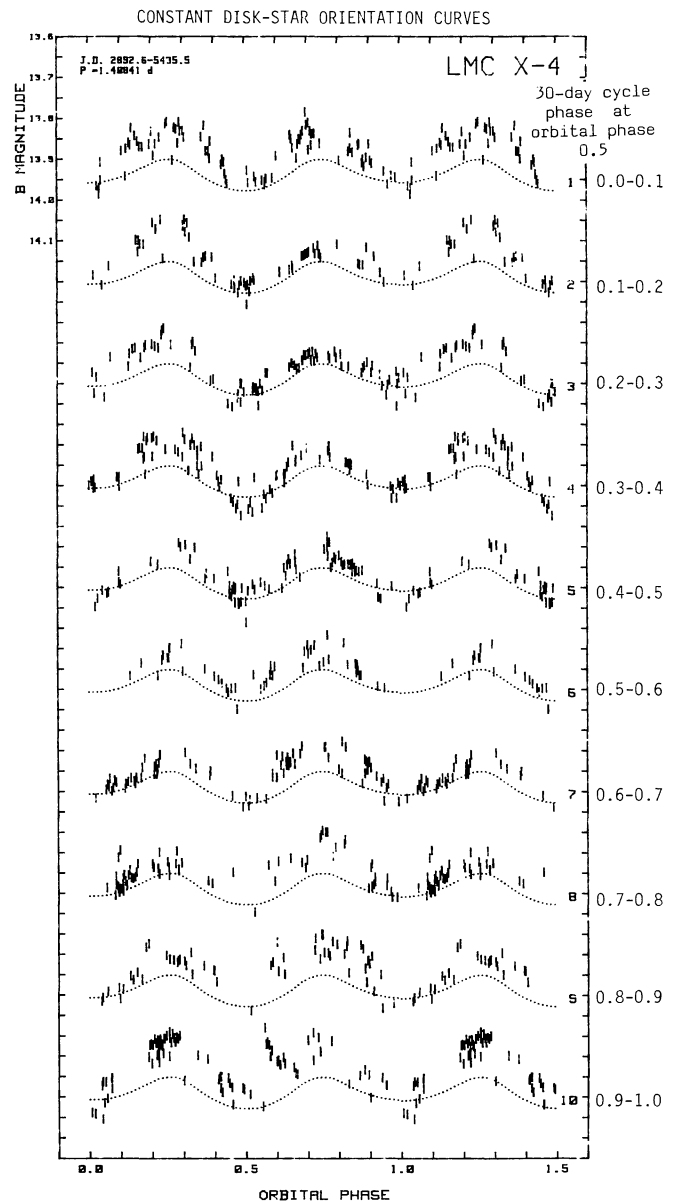


Fig. 4. Constant disk-star orientation light curves discussed in the text. Each curve corresponds to one of ten possible such orientations seen in a 30-d cycle. For a given curve, all 30-d phases seen by an Earth-bound observer corresponding to that disk-star orientation are sampled per “orbital” cycle. They were constructed by re-sampling the observed light curves shown in Fig. 3 along fixed orientation diagonals (draw an imaginary line which cuts each individual curve at successively earlier orbital phases so that all values are sampled in a 30-d cycle). Representative 30-d cycle phase intervals at orbital phase $\phi_{\text{orb}} = 0.5$ are given at right: 0.0–0.1 for curve 1, 0.1–0.2 for curve 2, . . . , and 0.9–1.0 for curve 10. The dotted curve superposed onto all light curves as a reference is the pure ellipsoidal model discussed in the text

effects of this illumination, and to separate it from the disk's own contribution, we have followed Gerend and Boynton (1976) by re-sampling the observed light curves shown in Fig. 3 along fixed orientation diagonals (draw an imaginary line which cuts each individual curve at successively earlier orbital phases so that all values are sampled in a 30-d cycle). This is equivalent to following a backward-moving feature in Fig. 3 with a period $P_2 = (f_2)^{-1} = 1.346 \text{ d}$. The results of this exercise are plotted in

Fig. 4. Each individual curve is labelled with the 30-d phase at orbital phase $\phi_{\text{orb}} = 0.5$. Each one of these elementary curves corresponds to given disk-star orientation, “frozen” for our convenience: looking at these curves as a function of ϕ_{orb} is equivalent to having the observer move “around” the binary system while the disk and the star keep their relative orientation fixed.

The first thing that strikes the eye in Fig. 4 is the *mirror-image symmetry* existing between curves 2–3 and curves 7–8: the $\phi_{\text{orb}} = 0.25$ and 0.75 maxima exchange roles. Obviously the disk-star configuration for $\phi_{\text{orb}} = 0.25$ in curves 2–3 is the same as that for $\phi_{\text{orb}} = 0.75$ in curves 7–8.

The mid-phase minimum deepens by 0.05 mag in curve 4 of Fig. 4, where the disk-star configuration corresponds to the X-ray ON state for an Earth-bound observer; the disk shows up under its most favorable conditions and, taking into account the inclination of the observer, passes in front of the primary, thereby causing a partial eclipse. The observed deficiency implies an apparent lower surface brightness for the disk.

In order to separate the disk from heated cap contributions, we now select a couple of disk-star configurations where, for our imaginary observer moving “around” the system, the disk’s contributions are identical, but the cap’s are different. In Fig. 4 such a couple is made up of curves 1 (or 10) and 5 at $\phi_{\text{orb}} = 0.25$ (or at $\phi_{\text{orb}} = 0.75$). Phase $\phi_{\text{orb}} = 0.5$ corresponds in curve 1 to the OFF state, with the disk seen almost edge-on, and in curve 5 to the ON state, the disk exposed as much as possible; moving “around” by a quarter of an orbital period exposes the disk by equal amounts, but still slightly edge-on for both configurations (remember, the observer is off the orbital plane by 24° !). In the first case it is oriented “towards” the Earth-bound observer, in the second “towards” the primary.

The contribution from the heated cap of the primary will differ radically in the two cases. In the first the disk shadow is projected on the upper half of the facing hemisphere and only the bottom half is illuminated, but as it lies “under” for us it will contribute very little. In the second case the disk will project its shadow on the bottom half of the facing hemisphere, which remains hidden for us anyway, while the X-rays will illuminate the upper half, seen sideways.

The difference between curves 1 (or 10) and 5 of Fig. 4 at $\phi_{\text{orb}} = 0.25$ is close to the maximum possible contribution³ from the illuminated cap of the companion, roughly about 0.05 mag, consistent with the amount of filling-in of the mid-orbital phase minimum (0.03–0.04 mag) observed during the OFF state (see Fig. 1 b). Note that this is *half* of the observed excess light present at quadratures in the ON state: the other half must come from the disk.

The mirror-image symmetry between curves 2–3 and curves 7–8 of Fig. 4 can be understood as follows: in curves 2–3 the disk is almost seen edge-on at $\phi_{\text{orb}} = 0.75$, and maximally exposed at $\phi_{\text{orb}} = 0.25$, while in curves 7–8 this situation is reversed. The cap’s contribution will *add* to the disk’s since (i) when the latter is seen edge-on, the shadow it projects on the primary “upper” side which faces Earth will be essentially all we see, and (ii) when it is seen at its best we also see the full contribution from the “upper” half of the illuminated cap. The addition of the two contributions in one case and near absence of both in the other thus explains the unequal maxima of curves 2–3 and 7–8.

3 The heated cap contribution may be slightly greater than the measured difference because the co-inclination is not very large and because of possible limb brightening

All other intermediate states of the curves seen in Fig. 4 can be explained by a mixture of disk and illuminated cap contributions.

10. Disk vs. cap contributions

A rough estimate can be made of the expected amount of X-ray radiation that should be reprocessed into *B*-band photons on the face of the primary and in the disk and compare them with the observed light excess. Taking a primary radius $R_{\text{opt}} = 8.9 R_\odot$, and a system separation of $a = 16 R_\odot$ (Kelley et al., 1983), the angle subtended by the companion as seen from the neutron star is $p = 2 \sin^{-1}(R/a) = 68^\circ$.

The luminosity due to reprocessing in the primary will be then:

$$L_h = L_x S (1 - b) (1 - k) g f,$$

where L_x is the total X-ray luminosity of the central source, $S = 0.5 (1 - \cos(p/2))$ is the fractional solid angle occupied by the primary as seen from the neutron star, b the X-ray albedo, g the bolometric factor (the luminosity coming out in the *B* band relative to the bolometric luminosity), f is a projection factor, and k the fraction of the X-ray flux effectively screened by the disk, which depends on its aspect as seen from the primary and on our viewing angle (k varies approximately between 0.1 and 0.4).

For the disk, approximated here as an axisymmetric flat plate of angular thickness $z = 20^\circ$, as in Her X-1, the luminosity will be:

$$L_d = 0.5 L_x \sin(z/2) (1 - b') g' f',$$

where b' and g' are the X-ray albedo and bolometric factor of the disk, and $f' = (0.6 \sin r + 0.4) \sin r$ is the projection factor for an incidence angle r ($r = 0^\circ$ when disk is viewed edge-on), including a limb-darkening term (Mihalas, 1981). The one-half comes from the fact that we see only one of its two faces at a given time.

We now estimate the maximum expected contributions from the heated cap and disk. For the heated cap, if $S = 0.084$, $b = 0.4$ (Milgrom and Salpeter, 1975; London et al., 1981), $g = 0.03$ (for a 35,000 K blackbody, Allen, 1973) and $k = 0.1$ we get $L_h = 1.4 \cdot 10^{-3} L_x f$. For the disk, $b' = 0.9$ (see van Paradijs, 1981) and $g' = 0.09$ (for a 25,000 K blackbody – see later – Allen, 1973), then $L_d = 8 \cdot 10^{-4} L_x f$, about the same maximum possible apparent luminosity as for the heated cap. Our main uncertainty lies in the value of b' , the X-ray albedo for large X-ray incidence angles.

The *B* band luminosity of the LMC X-4 primary is $L_B = 5 \cdot 10^{36} \text{ ergs}^{-1}$ (for $B_0 = 14.2$, $d = 55 \text{ kpc}$ and a 1000Å filter bandpass, Allen 1973) and $L_x = 7 \cdot 10^{38} \text{ ergs}^{-1}$ (2–80 keV, Kelley et al., 1983). At orbital phases 0.25 and 0.75 the projection factor f is < 0.2 (this includes limb-darkening) and consequently $L_h = 2 \cdot 10^{35} \text{ ergs}^{-1}$ or 4% of the primary’s *B* band luminosity. The disk, assuming a tilt angle of 20° (see above), makes an average $r = 40^\circ$ angle with respect to the line of sight, implying a projection factor < 0.5 . Then $L_d = 2.5 \cdot 10^{35} \text{ ergs}^{-1}$ or 5% of the primary’s *B* band luminosity. Assuming a smaller disk thickness z would decrease its maximum contribution relative to the heated cap’s. Within the uncertainties coming from the X-ray albedo, bolometric factor and disk thickness, we conclude that the heated cap of the primary or the heated disk can indeed each account for half the total excess light observed, about 10% of L_B , as is actually observed. As pointed out earlier, the smaller amplitude of the peak at the 30-d frequency is probably due to the inhomogeneous sampling of the long cycle.

Assuming the disk radiates the energy it absorbs as a black body, the effective temperature of the disk can be evaluated. The maximum size of the accretion can be computed by supposing it

fills its Roche lobe (this is not unreasonable, see Gerend and Boynton, 1976). We use the expression given by Paczynski (1971):

$$R_{\text{lobe}}/a = 0.462(q/(1+q))^{1/3},$$

where a is the semi-major axis and q the mass ratio. Taking $q = 0.1$ and $a = 16 R_{\odot}$, the X-ray source lobe radius is $R_{\text{lobe}} = 3.2 R_{\odot}$. This leads to $T_{\text{eff}} = 28,000$ K, close to the values reported for the quiescent optical temperature of the accretion disk in the X-ray burst source MXB 1636-53 (Lawrence et al., 1983), although this may be coincidental. If the extra deep mid-phase minimum observed during the ON state is due to a partial eclipse of the primary by the disk, we can check the consistency of the assumed system parameters. The B -band extra depth will be:

$$dL/L_B = \pi R_d^2 \sigma (T_*^4 g \sin r - T_d^4 g' f').$$

For $T_* = 35,000$ K, $T_d = 25,000$ K, $R_d = 3.2 R_{\odot}$, $g = 0.03$, $g' = 0.09$ and $r = 40^\circ$ we obtain $dL/L_B = 0.02$, a value compatible (within the large uncertainties in the above parameters) with the observed extra depth of 0.05 mag. Further modeling is probably not warranted by the present data.

11. Discussion

The X-ray and optical behaviour of the massive X-ray binary LMC X-4 imply the presence in this system of a “tilted” accretion disk undergoing apparent precession in a sense opposite to the orbital motion, as in Her X-1. The changes taking place in the light curve imply significant and roughly equal contributions from X-ray heating of the primary hemisphere facing the neutron star and from the accretion disk itself. This situation differs from that of Her X-1, where heating of the primary dominates by far.

Although tilted “precessing” accretion disks are required by the wealth of observational data available for both LMC X-4 and Her X-1, their true nature has been the subject of considerable discussion. (Katz, 1973; Roberts, 1974; Petterson, 1975, 1977a, b, 1978a, b; Merrit and Petterson, 1980; Papaloizou and Pringle, 1983). The clock responsible for the apparent precession in Her X-1, first thought to be real precession of the primary (Roberts, 1974), unexpected in this system (Papaloizou and Pringle, 1982), was later attributed to episodic mass transfer (Boynton et al., 1980); a process supported by the observations of X-ray dips during the “short-ON” state of Her X-1 by Gorecki et al. (1982) and by the analysis of optically reprocessed 1.24s pulsations in HZ Her (Middleditch, 1983). In this interpretation the disk precession is not “steady” but “apparent” due to the changing disk rim structure caused imposed by quasi-periodic mass transfers when the inner Lagrangian point L_1 is in the disk shadow (Crosa et al., 1980).

If the analogy with the Her X-1 system is complete, we expect to see in LMC X-4 X-ray dips marching with a period $P_2 = (f_{\text{orb}} + f_{\text{long}})^{-1} = 1.346$ -d. These would be due to occultation by the circulating disk rim structure, maintained by periodic accretion events taking place every 0.673 d, when the inner Lagrangian point is in the X-ray shadow cast by the disk, as in Her X-1 (Giacconi et al., 1973; Boynton et al., 1980). The quasi-periodic mass transfer is induced by the lack of X-ray radiation pressure on the inner Lagrangian point L_1 when it lies in the shadow of the disk. This pressure plays a fundamental role in the selection of the transferred material whose orbit nearly matches the tilt of the disk (Middleditch, 1983). It should however be stressed that the actual cause of the “tilt” and the long-period 35-d progression is still not known.

The 30-d X-ray curve is not asymmetric in LMC X-4, suggesting a radial disk profile different from that in Her X-1. In the latter the disk appears “twisted”, with its outer rim not coplanar with the inner regions (Petterson, 1975). This was introduced to account for the asymmetric ON-OFF cycle and the different spectral behavior seen during turn-ONs and turn-OFFs. During the former, changes in spectral shape suggest absorption by a cool, outer disk edge, while the lack of any such changes during turn-OFFs points to absorption by a hot, ionized inner disk region. This twisted shape is also consistent with expectations based on dynamical grounds (Merritt and Petterson, 1980). X-ray spectroscopic observations of LMC X-4 during the rising and declining branches should help in deciding whether a “twisted” disk is needed here.

A reappraisal remains to be done of the role of X-ray radiation pressure on mass transfer in LMC X-4, partly because of a somewhat smaller X-ray to optical luminosity ratio compared to Her X-1 and of the presence of a mild stellar wind, revealed by the phase-dependent absorption resonance lines of N v, C iv and Si iv and the accompanying hot ionized bubble around the X-ray source (Bonnet-Bidaud et al., 1981; van der Klis et al., 1982).

Further ultraviolet studies of LMC X-4 should allow a more precise determination of the accretion disk temperature and size. We note in passing that optically reprocessed 13s pulsations should be very difficult to detect due to the smaller X-ray amplitude and to the smaller heating effect, although the longer pulse period is a favorable factor.

Acknowledgements. We are indebted to ESO for the large amounts of observing time necessary for this long-term project. The La Silla staff are thanked for help with the instrumentation during the countless observing runs. Godelieve Hammerschlag-Hensberge provided the model light curves used here and we are very grateful for her collaboration. We thank L. Remijn, M. van der Klis, Th. van der Linden and others for the Dutch telescope observations they contributed. This work was started while C.M., M.P., and J.L. were at ESO, S.I., and C.C. at Observatoire de Paris-Meudon (LA 173).

Research at Besançon is supported by the CNRS (UA 389), MEN, INAG, and CNES.

References

- Allen, C.W.: 1973, *Astrophysical Quantities*, The Athlone Press, London
- Bonnet-Bidaud, J.M., Ilovaisky, S.A., Mouchet, M., Hammerschlag-Hensberge, G., van der Klis, M., Glencross, W.M., Willis, A.J.: 1981, *Astron. Astrophys.* **101**, 184
- Boynton, P.E., Crosa, L.M., Deeter, J.E.: 1980, *Astrophys. J.* **237**, 169
- Chevalier, C., Ilovaisky, S.A.: 1977, *Astron. Astrophys.* **59**, L9
- Chevalier, C., Ilovaisky, S.A., Motch, C., Pakull, M., Lub, J., van Paradijs, J.A.: 1981, *Spaces Sci. Revs.* **30**, 405
- Crosa, L., Boynton, P.E.: 1980, *Astrophys. J.* **235**, 999
- Davison, P.J.N., Fabian, A.: 1974, *Monthly Notices Roy. Astron. Soc.* **169**, 27P
- Deeter, J., Crosa, L., Gerend, D., Boynton, P.E.: 1976, *Astrophys. J.* **206**, 861
- Epstein, A., Delvaille, J., Helmken, H., Murray, S., Schnopper, H., Doxsey, R., Primini, F.: 1977, *Astrophys. J.* **216**, 103
- Gerend, D., Boynton, P.E.: 1976, *Astrophys. J.* **209**, 562
- Giacconi, R., Gursky, H., Kellog, E., Levinson, R., Schreier, E., Tananbaum, H.: 1973, *Astrophys. J.* **184**, 227

- Gorecki, A., Levine, A., Bautz, M., Lang, F., Primini, F.A., Lewin, W.H.G., Baity, W.A., Gruber, D.E., Rothschild, R.E.: 1982, *Astrophys. J.* **256**, 234
- Griffiths, R.E., Seward, F.D.: 1977, *Monthly Notices Roy. Astron. Soc.* **180**, 75P
- Hiltner, W.A.: 1977, *IAU Circ.* 3039
- Hutchings, J.B., Crampton, D., Cowley, A.P.: 1978, *Astrophys. J.* **225**, 548
- Hutchings, J.B.: 1982 in *Galactic X-Ray Sources*, Sanford, P., Laskarides, P., Salton, J. (Eds.), John Wiley and Sons, N.Y.
- Ilovaisky, S.A.: 1982 in *Galactic X-Ray Sources*, Sanford, P., Laskarides, P., Salton, J. (Eds.), John Wiley and Sons, N.Y.
- Johnson, H.: 1958, *Lowell Obs. Bull.* No. **90**, 37
- Jones, C., Forman, W.: 1976, *Astrophys. J. Letters* **209**, L131
- Kelley, R.L., Jernigan, J.G., Levine, A., Petro, L.D., Rappaport, S.A.: 1983, *Astrophys. J.* **264**, 568
- Kemp, J.C., Barbour, M.S., Henson, G.D., Kraus, D.J., Nolt, I.G., Radostitz, J.V., Priedhorsky, W.C., Terrell, J., Walker, E.N.: 1983, *Astrophys. J. Letters* **271**, L65
- van der Klis, M., Hammerschlag-Hensberge, G., Bonnet-Bidaud, J.M., Ilovaisky, S.A., Mouchet, M., Glencross, W.M., Willis, A.J., van Paradijs, J.A., Zuiderwijk, E.J., Chevalier, C.: 1981, *Astron. Astrophys.* **106**, 339
- Kurucz, R.L.: 1979, *Astrophys. J. Suppl.* **40**, 1
- Lang, F.L., Levine, A.M., Butz, M., Hauskins, S., Howe, S., Primini, F.A., Öewin, W.H.G., Baity, W.A., Knight, F.K., Rothschild, R.E., Petterson, J.A.: 1981, *Astrophys. J. Letters* **246**, L21
- Lawrence, A., Cominsky, L., Engelke, C., Jernigan, G., Lewin, W.H.G., Matsuoka, M., Mitsuda, K., Oda, M., Ohashi, T., Pedersen, H., van Paradijs, J.: 1983, *Astrophys. J.* **271**, 793
- Leong, Kellog, E., Gursky, H., Tananbaum, H., Giacconi, R.: 1971, *Astrophys. J. Letters* **170**, L67
- Li, F., Rappaport, S., Epstein, A.: 1978, *Nature* **271**, 37
- Lomb, H.R.: 1976, *Astrophys. Space Sci.* **39**, 447
- Markert, T.H., Clark, G.W.: 1975, *Astrophys. J. Letters* **196**, L55
- Merrit, D., Petterson, J.A.: 1980, *Astrophys. J.* **236**, 255
- Middleditch, J.: 1983, *Astrophys. J.* **275**, 140
- Mihalas, D.: 1978, *Stellar Atmospheres* (2nd ed.), W.H. Freeman & Co., San Francisco, p. 61
- Milgrom, M., Salpeter, E.E.: 1975, *Astrophys. J.* **196**, 583
- Motch, C.: 1979, Thesis, Université de Paris VI
- Pakull, M.: 1977, *IAU Circ.* 3017
- Papaloizou, J.C.B., Pringle, J.E.: 1982, *Monthly Notices Roy. Astron. Soc.* **200**, 49
- Papaloizou, J.C.B., Pringle, J.E.: 1983, *Monthly Notices Roy. Astron. Soc.* **202**, 1181
- van Paradijs, J.A.: 1978, *Astron. Astrophys. Suppl.* **29**, 339
- van Paradijs, J.: 1981, *Astron. Astrophys.* **103**, 140
- van Paradijs, J., Zuiderwijk, E.: 1977, *Astron. Astrophys.* **61**, L19
- Paczynski, B.: 1971, *Ann. Rev. Astron. Astrophys.* **9**, 183
- Petterson, J.A.: 1975, *Astrophys. J. Letters* **201**, L61
- Petterson, J.A.: 1977a, *Astrophys. J.* **214**, 550
- Petterson, J.A.: 1977b, *Astrophys. J.* **218**, 783
- Petterson, J.A.: 1978a, *Astrophys. J.* **224**, 625
- Petterson, J.A.: 1978b, *Astrophys. J.* **226**, 253
- Priedhorsky, W.C., Terrell, J.: 1983, *Astrophys. J.* (in press)
- Priedhorsky, W.C., Terrell, J., Holt, S.S.: 1983, *Astrophys. J.* **270**, 233
- Rapley, C.G., Touhy, I.R.: 1974, *Astrophys. J. Letters* **191**, L113
- Sanduleak, N., Philip, A.G.D.: 1977, *IAUC* 3023
- Skinner et al.: 1980, *Astrophys. J.* **240**, 619
- Tuohy I.R., Rapley, C.G.: 1975, *Astrophys. J. Letters* **198**, L69
- White, N.E.: 1978, *Nature* **271**, 38
- Zuiderwijk, E.J., Hammerschlag-Hensberge, G., van Paradijs, J., Sterken, C., Hensberge, H.: 1977, *Astron. Astrophys.* **54**, 167